applied sciences

MDPI

Article

Target Localization in Underwater Acoustic Sensor Networks Using RSS Measurements

Shengming Chang [1], Youming Li [1,*], Yucheng He [2] and Hui Wang [1]

1 Faculty of Electrical Engineering and Computer Science, Ningbo University, Ningbo 315211, China; csm20130504@163.com (S.C.); wangh0802@163.com (H.W.)
2 Xiamen Key Laboratory of Mobile Multimedia Communications, Huaqiao University, 668 Jimei Avenue, Xiamen 361021, China; yucheng.he@hqu.edu.cn
* Correspondence: liyouming@nbu.edu.cn; Tel.: +1-885-749-6387

Received: 28 November 2017; Accepted: 29 January 2018; Published: 1 February 2018

Abstract: This paper addresses the target localization problems based on received signal strength (RSS) measurements in underwater acoustic wireless sensor network (UWSN). Firstly, the problems based on the maximum likelihood (ML) criterion for estimating target localization in cases of both known and unknown transmit power are respectively derived, and fast implementation algorithms are proposed by transforming the non-convex problems into a generalized trust region subproblem (GTRS) frameworks. A three-step procedure is also provided to enhance the estimation accuracy in the unknown target transmit power case. Furthermore, the Cramer–Rao lower bounds (CRLBs) in both cases are derived. Computer simulation results show the superior performance of the proposed methods in the underwater environment.

Keywords: underwater acoustic wireless sensor network (UWSN); target localization; received signal strength (RSS); Cramer–Rao lower bounds (CRLBs)

1. Introduction

Target localization in underwater acoustic wireless sensor network (UWSN) has attracted much attention in recent years due to its wide applications in such fields as data collection, pollution monitoring, offshore exploration, disaster prevention, target tracking, assisted navigation, and military surveillance [1–3]. In UWSN, target localization is often performed by using such measurement information as time-of-arrival (ToA), time-different-of-arrival (TDoA), angle-of-arrival (AoA), and received-signal-strength (RSS). However, localization based on ToA and TDoA requires careful timing and synchronization, and the costs are high, especially in underwater acoustic environmental conditions [4–6]. Additionally, as AoA relies on a direct line-of-sight path from the target node to anchor nodes, it will cause large errors in AoA measurements in multi-path underwater acoustic (UWA) transmission environments [7,8]. Therefore, RSS-based target localization is preferred by researchers due to its low complexity and easy implementation [9–12]. Based on the received signal strength measurements, the maximum likelihood (ML) method is used to estimate the target position [13], and this method is robust in underwater environments. Although the ML estimator has asymptotically optimal performance, it is non-convex and has multiple local optimal solutions. Moreover, its performance depends highly on the initial solution and obtains bad results if a poor initialization is provided. In [9], the authors propose a fast iteration algorithm by using a triangulation method based on RSS measurements. In [11], the authors discuss the convex optimization method for target localization in UWSN, while the propagation model is still the terrestrial acoustic wave model. Two convex methods based respectively on RSS-based and frequency-dependent differential approaches in UWSN have been proposed [12]. A hybrid localization method was investigated by combining ToA and RSS measurements [10]. This method provides better performance by exploiting the benefits of combined measurements of the radio signal in the assumption that the RSS measurements are known in advance.

In this paper, target localization methods for the cases of both known and unknown target transmit power are proposed. Firstly, the general target localization problems based on the ML criterion are formed, and the new weighted least square (WLS) problems are then derived using approximation techniques. These non-convex estimators are then transformed into a generalized trust region subproblem (GTRS) framework [14], which are solved in an efficient way. Furthermore, a three-step procedure is used to enhance the estimation accuracy of the target localization in the unknown target transmit power case. Finally, the closed-form expressions of the Cramer–Rao lower bounds (CRLBs) in both known and unknown target transmit power cases are derived.

The remainder of this paper is organized as follows. In Section 2, the RSS measurement model for locating a single target node is briefly introduced, and the non-convex target localization problem is formulated. Section 3 derives the proposed methods in both the known and unknown transmit power cases. In Section 4, complexity analysis is carried out. Computer simulation comparisons of the discussed methods are presented in Section 5. The CRLBs in both known and unknown transmit power cases are derived in Section 6. In Section 7, the main conclusions are drawn. Finally, Section 8 points out the idea of further research.

2. The System Model

Consider an UWSN with N anchor nodes and one target node in a two-dimensional ($2D$) localization scenario, where the locations of anchor nodes, noted as $\boldsymbol{s}_1, \boldsymbol{s}_2, \ldots, \boldsymbol{s}_N$, are known, while the location of the target node, noted as $\boldsymbol{x}$, is unknown. For simplicity and without loss of generality, we assume that the anchor nodes are equipped with omnidirectional antennas. Under a centralized processing mode, all sensors convey their RSS measurements with respect to the target node to the central processor. We assume that the locations of all the nodes are supposed to be unchanged during the computation period [11,15]. Figure 1 shows the i-th sensoring link in the UWSN model.

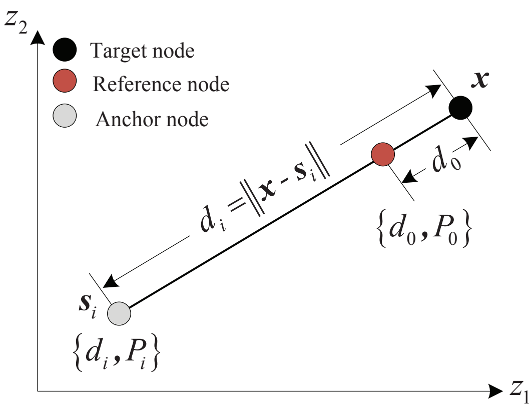

Figure 1. The i-th sensoring link in the underwater acoustic wireless sensor network (UWSN) model.

For $i = 1, 2, \ldots, N$, the RSS of the UWA propagation between the i-th anchor node and the target node is measured in dBm and has the log-normal shadowing model as follows [12]:

$$P_i = P_0 - 10\gamma \log_{10} \frac{d_i}{d_0} - \alpha_f (d_i - d_0) + n_i \tag{1}$$

where $d_i = \|\boldsymbol{x} - \boldsymbol{s}_i\|$ is the Euclidean distance, n_i is a zero-mean Gaussian random variable with covariance matrix $\boldsymbol{Q}$ that represents the log-normal shadowing effect, P_0 is the reference power at the reference distance $d_0 (d_0 \leq d_i)$, γ is the path-loss exponent between 2 and 4 according to different propagation environments, and α_f is the absorption coefficient that can be obtained from Thorp's formula as a function of signal frequency f in dB/km, which is as follows [16]:

$$\alpha_f = \frac{0.11 f^2}{1+f^2} + \frac{44 f^2}{4100+f^2} + 2.75 \times 10^{-4} f^2 + 0.003. \tag{2}$$

Let $\boldsymbol{n} = (n_1, n_2, \ldots, n_N)^T \in \mathbb{R}^N$ be the collection vector of Gaussian random variables with a symmetric and positive-definite covariance matrix $\boldsymbol{Q}$ as follows:

$$[\boldsymbol{Q}]_{ij} = \begin{cases} \sigma^2, & i = j \\ \rho\sigma^2, & i \neq j \end{cases} \tag{3}$$

where $0 \leq \rho < 1$ is the correlation coefficient of any two different links between i and j to the target node for $i, j = 1, 2, \ldots, N$. It is known from Equation (3) that $\boldsymbol{Q}$ can be transformed into white noise using the Cholesky decomposition as $\boldsymbol{Q} = \boldsymbol{B}\boldsymbol{B}^T$ with lower-triangular matrix $\boldsymbol{B}$. This implies a linear transformation $\boldsymbol{n} = \boldsymbol{B}\boldsymbol{w}$, where $\boldsymbol{w} \sim \mathcal{N}(\boldsymbol{0}, \sigma^2 \boldsymbol{I}_N)$, and $\boldsymbol{I}_N$ is the order-N unity matrix [17].

Let $\boldsymbol{P} = (P_1, P_2, \cdots, P_N)^T \in \mathbb{R}^N$ be the vector of observations given by Equation (1). The joint probability density function (PDF) of $\boldsymbol{P}$, conditioned on a given $\boldsymbol{x}$, has the following form

$$f(\boldsymbol{P}|\boldsymbol{x}) = \frac{1}{(2\pi)^{\frac{N}{2}} |\boldsymbol{Q}|^{\frac{1}{2}}} e^{-\frac{1}{2}\left(\boldsymbol{P}-\widehat{\boldsymbol{P}}\right)^T \boldsymbol{Q}^{-1}\left(\boldsymbol{P}-\widehat{\boldsymbol{P}}\right)} \tag{4}$$

where $\widehat{\boldsymbol{P}} = \left(\widehat{P}_1, \widehat{P}_2, \ldots, \widehat{P}_N\right)^T$, with each component

$$\widehat{P}_i = P_0 - 10\gamma \log_{10} \frac{\|\boldsymbol{x} - \boldsymbol{s}_i\|}{d_0} - \alpha_f(\|\boldsymbol{x} - \boldsymbol{s}_i\| - d_0).$$

Therefore, the joint ML estimation of the target location $\boldsymbol{x}$ can be formulated as

$$\arg\min_{\boldsymbol{x}} \; (\boldsymbol{P} - \widehat{\boldsymbol{P}})^T \boldsymbol{Q}^{-1} (\boldsymbol{P} - \widehat{\boldsymbol{P}}). \tag{5}$$

In the special case where $\rho = 0$, which corresponds to added white Gaussian noise, the estimation can be reduced as

$$\arg\min_{\boldsymbol{x}} \sum_{i=1}^{N} \left(P_i + 10\gamma \log_{10} \|\boldsymbol{x} - \boldsymbol{s}_i\| + \alpha_f \|\boldsymbol{x} - \boldsymbol{s}_i\| - P_0 - 10\gamma \log_{10} d_0 - \alpha_f d_0\right)^2. \tag{6}$$

Clearly, the ML estimator based on Equation (5) or Equation (6) is non-convex, hence the difficulty in finding a global optimal solution.

3. The Proposed Methods

In this section, we provide an approximation method that can transform the ML estimator into a GTRS problem. Without loss of generality, we assume that noise n_i is sufficiently small, and let $d_0 = 1$ m [12,15]. From Equation (1), we have the following approximation expression

$$\|\boldsymbol{x} - \boldsymbol{s}_i\| \approx 10^{\frac{P_0 - P_i + \alpha_f}{10\gamma}} 10^{-\frac{\alpha_f \|\boldsymbol{x} - \boldsymbol{s}_i\|}{10\gamma}}. \tag{7}$$

Let $u = -\frac{\alpha_f \|\boldsymbol{x} - \boldsymbol{s}_i\|}{10\gamma}$ be the exponent of the second factor on the right hand side of Equation (7). It was shown in [12,18] that, when the absorption coefficient α_f is sufficiently small, the absorption term $\alpha_f \|\boldsymbol{x} - \boldsymbol{s}_i\|$ can be relatively small ($\alpha_f \|\boldsymbol{x} - \boldsymbol{s}_i\| \ll \frac{10\gamma}{\ln 10}$), especially in deep water; then, $0 < |u| \ll 1$.

Therefore, for a sufficiently small α_f, it is reasonable to approximate this factor by using the first-order Taylor expansion about $u = 0$ as follows:

$$10^{-\frac{\alpha_f \|\boldsymbol{x}-\boldsymbol{s}_i\|}{10\gamma}} \approx 1 - \ln 10 \cdot \frac{\alpha_f \|\boldsymbol{x}-\boldsymbol{s}_i\|}{10\gamma} \tag{8}$$

where the higher-order terms are omitted.

By substituting Equation (8) into Equation (7), the distance between the i-th anchor and the target node can be further approximated in the following form:

$$\lambda_i \|\boldsymbol{x}-\boldsymbol{s}_i\| \approx \eta, \tag{9}$$

where $\lambda_i = \beta_i + \frac{\eta \alpha_f \ln 10}{10\gamma}$ $\beta_i = 10^{\frac{P_i - \alpha_f}{10\gamma}}$, and $\eta = 10^{\frac{P_0}{10\gamma}}$.

3.1. Target Localization in the Known Transmit Power Case

In the known transmit power case, P_0 is assumed to be known in the centralized localization, so η is a constant that depends only on the path-loss exponent γ. Given γ, α_f, $\{P_i\}_{i=1}^N$, and the coefficients $\{\lambda_i\}_{i=1}^N$, the target node localization can be determined from Equation (9). Next, we can rewrite Equation (9) as

$$\lambda_i^2 \|\boldsymbol{x}-\boldsymbol{s}_i\|^2 \approx \eta^2. \tag{10}$$

Based on Equation (10), we propose the following WLS estimation problem:

$$\min_{\boldsymbol{x}} \sum_{i=1}^{N} (\lambda_i^2 \|\boldsymbol{x}-\boldsymbol{s}_i\|^2 - \eta^2)^T \boldsymbol{Q}^{-1} (\lambda_i^2 \|\boldsymbol{x}-\boldsymbol{s}_i\|^2 - \eta^2). \tag{11}$$

The above WLS estimator is still a non-convex optimization problem. In the following section, we can transform Equation (11) into an equivalent quadratic programming problem with a quadratic constraint whose global solution can be computed efficiently [19].

Let $\boldsymbol{y} = \left[\boldsymbol{x}^T, \|\boldsymbol{x}\|^2\right]^T$, and Equation (11) can be written in an equivalent GTRS problem as

$$\begin{aligned} &\min_{\boldsymbol{y}} \ \|\boldsymbol{Q}^{-\frac{1}{2}}(\boldsymbol{A}\boldsymbol{y}-\boldsymbol{b})\|^2 \\ &\text{s.t.} \ \ \boldsymbol{y}^T\boldsymbol{D}\boldsymbol{y} + 2\boldsymbol{v}^T\boldsymbol{y} = 0 \end{aligned} \tag{12}$$

where $\boldsymbol{D} = diag([1,1,0]), \boldsymbol{v} = [0,0,-\frac{1}{2}]^T$, and

$$\boldsymbol{A} = \begin{bmatrix} -2\lambda_1^2 s_1^T & \lambda_1^2 \\ \vdots & \vdots \\ -2\lambda_N^2 s_N^T & \lambda_N^2 \end{bmatrix}, \boldsymbol{b} = \begin{bmatrix} \eta^2 - \lambda_1^2 \|\boldsymbol{s}_1\|^2 \\ \vdots \\ \eta^2 - \lambda_N^2 \|\boldsymbol{s}_N\|^2 \end{bmatrix}. \tag{13}$$

Although Equation (12) is still non-convex, both the objective function and the constraint in Equation (12) are quadratic. This is a typical quadratic programming problem with quadratic constraint and can be solved using the bisection method [19]. In the sequel, this method is noted as "WLS-K"(weighted least square–known).

3.2. Target Localization in the Unknown Transmit Power Case

In most practical applications, the target transmit power is unknown. Therefore, the related P_0 or η in Equation (11) is unknown. Therefore, the method proposed in Section 3.1 cannot be used directly in this case. To cope with the difficulties caused by this additional unknown parameter, we developed the following method.

By using the notations of λ_i, β_i and η, from Equation (9), we have

$$\|\boldsymbol{x} - \boldsymbol{s}_i\| \approx \frac{\eta}{\beta_i + \frac{\alpha_f \ln 10}{10\gamma}\eta} \tag{14}$$

and thus

$$\|\boldsymbol{x} - \boldsymbol{s}_i\| \approx \frac{\frac{10\gamma}{\alpha_f \ln 10}(\beta_i + \frac{\alpha_f \ln 10}{10\gamma}\eta) - \frac{10\gamma}{\alpha_f \ln 10}\beta_i}{\beta_i + \frac{\alpha_f \ln 10}{10\gamma}\eta}. \tag{15}$$

Furthermore, Equation (15) can be rewritten as

$$\|\boldsymbol{x} - \boldsymbol{s}_i\| \approx \frac{10\gamma}{\alpha_f \ln 10} - \frac{\frac{10\gamma}{\alpha_f \ln 10}\beta_i}{\beta_i + \frac{\alpha_f \ln 10}{10\gamma}\eta}. \tag{16}$$

We divide β_i from both the numerator and denominator of the second term on the right hand side of Equation (16), yielding

$$\|\boldsymbol{x} - \boldsymbol{s}_i\| \approx \frac{10\gamma}{\alpha_f \ln 10} - \frac{10\gamma}{\alpha_f \ln 10} \cdot \frac{1}{1 + \frac{\alpha_f \ln 10}{10\gamma} \cdot \frac{\eta}{\beta_i}}. \tag{17}$$

Let $\nu = \frac{\alpha_f \ln 10}{10\gamma\beta_i}\eta$, in which α_f is related to the frequency, β_i is related to the signal power, γ is a constant, and η is an independent unknown parameter. We will verify that $|\nu| \ll 1$ in most UWSN environments. Figure 2 is the α_f versus the frequency band 0–30 kHz, within which most acoustic systems operate [20–22]. The figure shows that $\alpha_f \ll 1$. Figure 3 shows ν versus the transmit signal power when α_f takes three different values (in dB/m). The figure shows that $|\nu| \ll 1$ in this case. Therefore, when the absorption coefficient α_f is sufficiently small, it is reasonable to approximate Equation (17) by using the first-order Taylor expansion about $\nu = 0$ as follows:

$$\frac{1}{1 + \frac{\alpha_f \ln 10}{10\gamma} \cdot \frac{\eta}{\beta_i}} \approx 1 - \frac{\alpha_f \ln 10}{10\gamma} \cdot \frac{\eta}{\beta_i}. \tag{18}$$

Taking Equation (18) into Equation (17), we have the following simplified form:

$$\|\boldsymbol{x} - \boldsymbol{s}_i\| \approx \frac{\eta}{\beta_i}. \tag{19}$$

As in the previous section, squaring both sides of Equation (19), we have

$$\|\boldsymbol{x} - \boldsymbol{s}_i\|^2 \approx \frac{\eta^2}{\beta_i^2}. \tag{20}$$

Thus, we can obtain the following WLS problem:

$$\min_{\boldsymbol{x},\eta} \sum_{i=1}^{N} (\|\boldsymbol{x} - \boldsymbol{s}_i\|^2 - \frac{\eta^2}{\beta_i^2})^T \boldsymbol{Q}^{-1} (\|\boldsymbol{x} - \boldsymbol{s}_i\|^2 - \frac{\eta^2}{\beta_i^2}). \tag{21}$$

Let $\widetilde{\boldsymbol{y}} = \left[\boldsymbol{x}^T, \|\boldsymbol{x}\|^2, \eta, \eta^2\right]^T$, and Equation (21) can be written in equivalent GTRS form as

$$\begin{aligned} &\min_{\widetilde{\boldsymbol{y}}} \ \|\boldsymbol{Q}^{-\frac{1}{2}}(\widetilde{\boldsymbol{A}}\widetilde{\boldsymbol{y}} - \widetilde{\boldsymbol{b}})\|^2 \\ &\text{s.t.} \ \ \widetilde{\boldsymbol{y}}^T\widetilde{\boldsymbol{D}}\widetilde{\boldsymbol{y}} + 2\widetilde{\boldsymbol{v}}^T\widetilde{\boldsymbol{y}} = 0 \end{aligned} \tag{22}$$

where $\widetilde{\boldsymbol{D}} = diag([1,1,0,1,0]), \widetilde{\boldsymbol{v}} = [0,0,-\frac{1}{2},0,-\frac{1}{2}]^T$, and

$$\widetilde{\boldsymbol{A}} = \begin{bmatrix} -2s_1^T & 1 & 0 & -\frac{1}{\beta_1^2} \\ \vdots & \vdots & \vdots & \vdots \\ -2s_N^T & 1 & 0 & -\frac{1}{\beta_N^2} \end{bmatrix}, \widetilde{\boldsymbol{b}} = \begin{bmatrix} -\|\boldsymbol{s}_1\|^2 \\ \vdots \\ -\|\boldsymbol{s}_N\|^2 \end{bmatrix}. \tag{23}$$

Equation (22) is still non-convex, but both the objective function and the constraint are quadratic and can therefore be solved by using the bisection method [19], as discussed in Section 3.1.

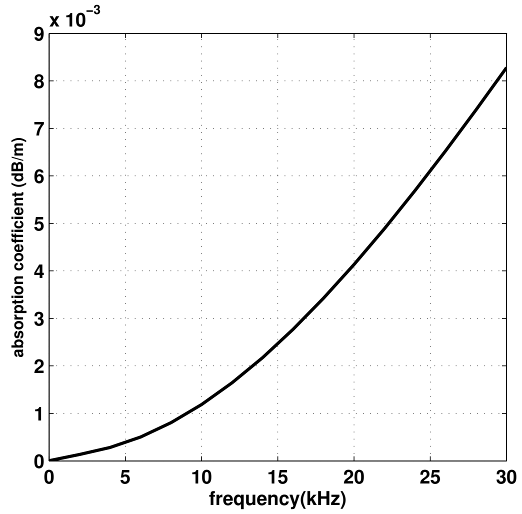

Figure 2. Absorption coefficient, α_f, versus frequency.

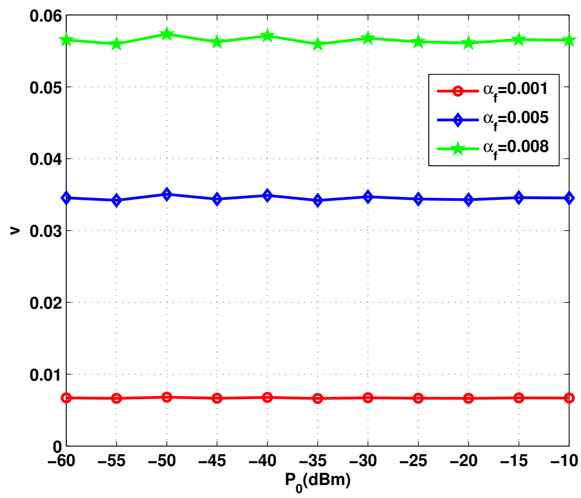

Figure 3. $\nu = \frac{\alpha_f \ln 10}{10\gamma\beta_i}\eta$ versus the transmit power P_0 in Equation (18) for several α_f.

In fact, we can further improve localization performance in the unknown transmit power case. To do so, first, we solve Equation (22) to obtain the initial location estimate of target node $\boldsymbol{x}$, $\widehat{\boldsymbol{x}}_1$, and then use this estimate to search for the ML estimate of the transmit power P_0, $\widehat{P}_0$. Finally, with the estimated $\widehat{P}_0$, the problem is transformed into the localization in the known transmit power case. Hence, we form the following three-step procedure:

(1) Solve Equation (22) to obtain an initial estimate of $\boldsymbol{x}$, $\widehat{\boldsymbol{x}}_1$.

(2) Use $\widehat{\boldsymbol{x}}_1$ to search for the ML estimate of P_0, $\widehat{P}_0$ as

$$\widehat{P}_0 = \frac{\sum_{i=1}^{N}(P_i + 10\gamma\log_{10}\frac{\widehat{d}_i}{d_0} + \alpha_f(\widehat{d}_i - d_0))}{N} \tag{24}$$

where $\widehat{d}_i = \|\widehat{\boldsymbol{x}}_1 - \boldsymbol{s}_i\|$.

(3) Use $\widehat{P}_0$ to calculate the $\widehat{\eta} = 10^{\frac{\widehat{P}_0}{10\gamma}}, \widehat{\lambda}_i = \beta_i + \frac{\widehat{\eta}\alpha_f \ln 10}{10\gamma}$ and use this estimate to solve the WLS-K in Equation (12), then obtain the new estimate of $\boldsymbol{x}$, $\widehat{\boldsymbol{x}}$.

We label this method as "WLS-U"(weighted least square–unknown).

4. Complexity Analysis

There is an inherent trade-off between estimation accuracy and implementation complexity among all proposed methods. The method for the *worst-case* complexity of the mixed SD/SOCP [23] is used to analyze the complexities of the proposed and other discussed methods in this paper. Table 1 shows that the computational complexity of the discussed methods mainly depend on the network size, i.e., the number of anchor nodes.

Table 1. Summary of the considered methods.

Method	Description	Complexity
SDP (semi–definite programming)	RSS-based SDP method in [12]	$\mathcal{O}(N^{3.5})$
WLS-K (weighted least square-known)	The proposed WLS-K Equation (13)	$\mathcal{O}(K_{max}N)$
WLS-U (weighted least square-unknown)	The proposed WLS-U Equation (22)	$2\mathcal{O}(K_{max}N)$

From Table 1, we see that the proposed methods have less complexity.

5. Cramer–Rao Lower Bound Analysis

The Cramer–Rao lower bounds of the target localization in UWSN are derived in this section to compare the performance of the proposed methods. Let $\boldsymbol{B}_1 = (\boldsymbol{G}^T\boldsymbol{Q}^{-1}\boldsymbol{G})^{-1}$, and $\boldsymbol{B}_2 = (\boldsymbol{H}^T\boldsymbol{Q}^{-1}\boldsymbol{H})^{-1}$, where $\boldsymbol{G} = [g_1, g_2, \cdots, g_N]^T$, and $\boldsymbol{H} = [h_1, h_2, \cdots, h_N]^T$, with

$$g_i = -\frac{10\gamma}{ln10}\frac{(\boldsymbol{x}-\boldsymbol{s}_i)^T}{\|\boldsymbol{x}-\boldsymbol{s}_i\|^2} - \alpha_f\frac{(\boldsymbol{x}-\boldsymbol{s}_i)^T}{\|\boldsymbol{x}-\boldsymbol{s}_i\|}, i = 1,\ldots,N \tag{25}$$

$$h_i = [-\frac{10\gamma}{ln10}\frac{(\boldsymbol{x}-\boldsymbol{s}_i)^T}{\|\boldsymbol{x}-\boldsymbol{s}_i\|^2} - \alpha_f\frac{(\boldsymbol{x}-\boldsymbol{s}_i)^T}{\|\boldsymbol{x}-\boldsymbol{s}_i\|}, 1]^T, i = 1,\ldots,N. \tag{26}$$

Thus, the Cramer-Rao lower bounds (CRLBs) of the target node location $\boldsymbol{x}$ in both known and unknown transmit power cases, i.e., CRLB-K (Cramer–Rao lower bound-known) and CRLB-U (Cramer–Rao lower bound-unknown) can respectively be written as

$$\text{CRLB-K}(\boldsymbol{x}) = \text{trace}(\boldsymbol{B}_1) \tag{27}$$

$$\text{CRLB-U}(\boldsymbol{x}) = \text{trace}(\boldsymbol{B}_2[1{:}2, 1{:}2]). \tag{28}$$

For detailed derivations, please refer to the Appendix.

6. Simulation Results and Analysis

In this section, computer simulation results are used to compare the performance of the proposed methods with the SDP method (RSS-based approach) in [12] in underwater acoustic environments. The propagation model, Equation (1), is used to generate the range measurements. The anchor nodes and target node are assumed to be randomly located at a square region 100 m $\times$ 100 m in each Monte carlo (Mc) run. Unless otherwise stated, the reference distance is set to be $d_0 = 1$ m, the reference power is $P_0 = -10$ dBm, the maximum number of steps in the bisection procedure is $K_{max} = 30$, and the path-loss exponent is fixed as $\gamma = 2$, which corresponds to an UWA spherical spreading case. Different values of α_f are given in each figure. The noise correlation coefficient $\rho = 0.8$ for $i \neq j$. Three thousand Monte carlo runs are used to compute the root mean square error (RMSE) defined as RMSE$=\sqrt{\sum_{i=1}^{Mc} \frac{\|x - \hat{x}\|^2}{Mc}}$, where $\hat{x}$ is the estimated location in the i-th Monte Carlo run. The SDP is solved using the MATLAB package CVX (Version 2.1, Stanford University, Stanford, CA, USA, 2014) [24], where the solver is SeDuMi (Version 1.02, Tilburg University, Tilburg, Netherlands, 1999) [25]. The corresponding ML problems are solved by the MATLAB function "Isqnonlin," which adopts the Levenberg–Marquardt algorithm.

Figure 4 compares the RMSE versus the standard derivation σ. It is observed that the RMSE grows in nature as the standard derivation increases for all the methods. The proposed localization method WLS-K in the case of known transmit power provides superior performance over the SDP method, and approximates the CRLB-K even when the standard derivation increases. Furthermore, to the best of the authors' knowledge, few people has discussed localization methods based on a UWA RSS propagation model in unknown transmit power cases in UWSN. Therefore, we compared the performance of the proposed WLS-U with CRLB-U in this case. The results show that the proposed method in this case also maintains an optimal performance.

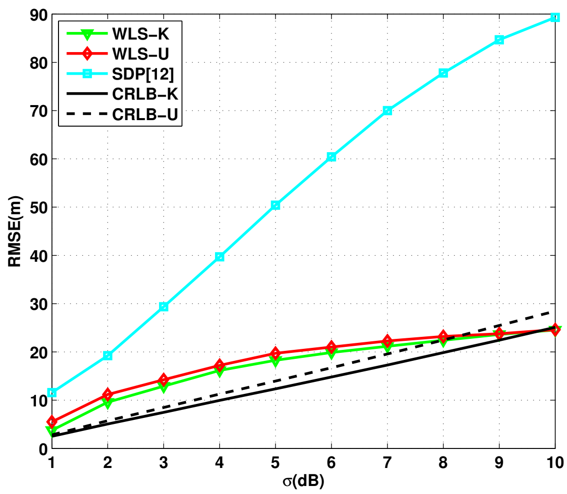

Figure 4. Root mean square error (RMSE) versus the σ when N = 10, α_f = 0.001 dB/m (f = 9 kHz), and ρ = 0.8.

Figure 5 compares the RMSE versus the number N of the anchor nodes. As predicted, the RMSE decreases in nature as N increases for both the WLS-K and WLS-U methods. The figure also shows that adding more anchor nodes in the network can enhance the performance of the proposed methods and outperform the SDP method for all chosen N. Moreover, the performance of WLS-K is slightly better than WLS-U.

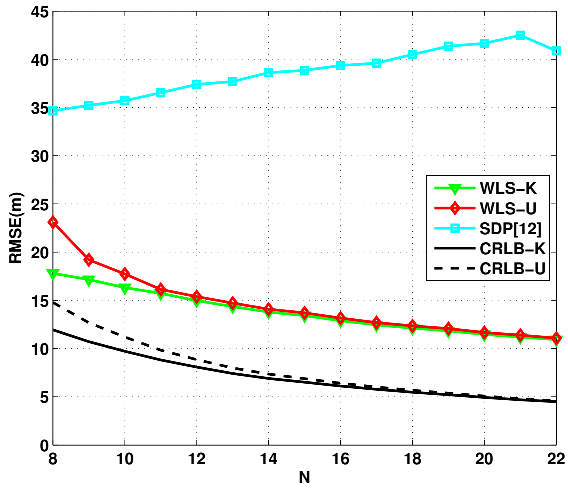

Figure 5. RMSE versus the anchor node number N when σ = 4 dB, α_f = 0.01 dB/m (f = 34 kHz), and ρ = 0.8.

Figure 6 depicts the cumulative density function (CDF) of localization comparison versus mean error (ME) among the discussed methods. The figure shows that the proposed methods show an improvement in performance compared with the SDP method.

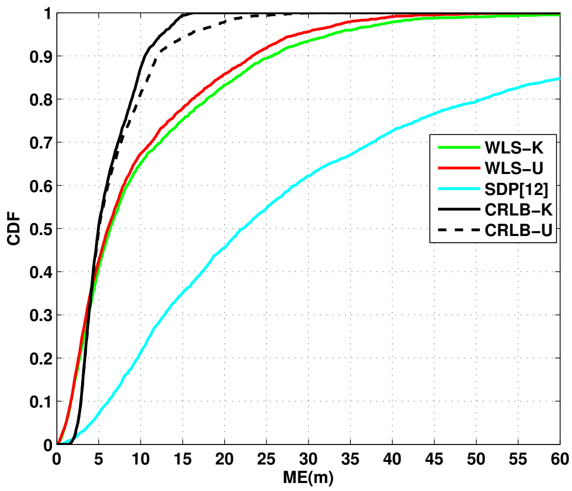

Figure 6. Cumulative density function (CDF) versus mean error (ME) when σ = 4 dB, α_f = 0.1 dB/m (f = 454 kHz), N = 10, and ρ = 0.8.

Figure 7 compares the RMSE versus the absorption coefficient α_f. The figure shows that the RMSE crease in with the increase in absorption coefficient for the discussed methods, and WLS-K method shows a performance that is superior to the SDP method. Furthermore, the gap between the WLS-K method and the WLS-U method is small. This is due to the fact that, in the proposed WLS-U method, with some approximation, the unknown transmit power P_0 can be estimated from the GTRS optimization problem, Equation (22). In this case, the problem is transformed into the same problem in the known transmitter power case. The results show that the proposed methods have robust performance for α_f from 0.001 to 0.1 dB/m.

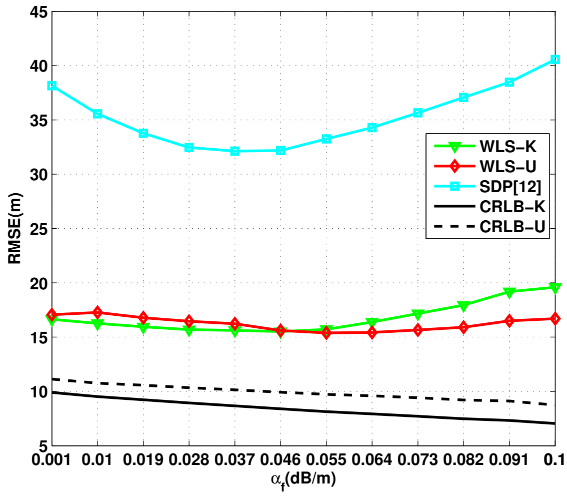

Figure 7. RMSE versus absorption coefficient α_f when $\sigma = 4$ dB, $N = 10$, and $\rho = 0.8$.

Figure 8 illustrates the RMSE versus transmit power P_0. The figure shows that the RMSE of the discussed methods maintains a robust performance with the change in transmit power. Moreover, like the WLS-K method, the proposed WLS-U method also shows a superior performance for P_0 from -60 to -10 dBm.

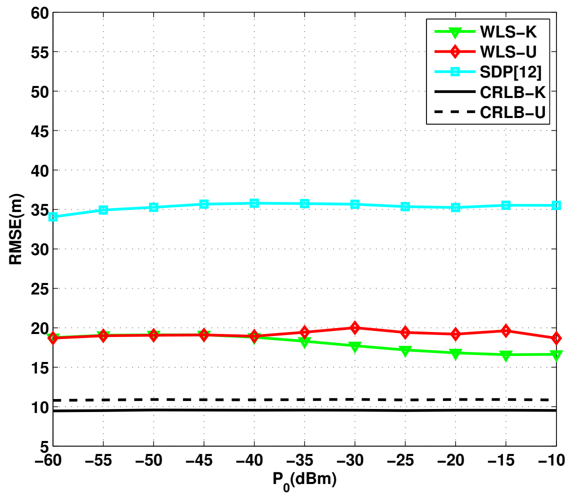

Figure 8. RMSE versus transmit power P_0 when $\sigma = 4$ dB, $\alpha_f = 0.01$ dB/m ($f = 34$ kHz), $N = 10$, and $\rho = 0.8$.

7. Conclusions

In this paper, the target localization problems using RSS measurements in UWSN in both known and unknown transmit power cases are investigated. Firstly, an optimization problem for estimating target localization in both cases is presented. The derived objective function is then transformed into a GTRS framework. Efficient implementation methods are provided in both known and unknown target transmit power cases. The closed-form expressions of the CRLBs in both cases are derived. Computer simulation results confirm the effectiveness of the proposed methods in underwater acoustic environments.

8. Further Research

This study was limited to a stationary environment where the anchor and target node positions are unchanged during the observation period. In most UWSN environments, however, the positions of the target or anchor nodes change. Therefore, the localization method for mobile nodes in UWSN should be studied.

Acknowledgments: The authors gratefully acknowledge the grants from the National Natural Science Foundation of China (61571250), the Ningbo Natural Science Foundation(2015A610121), the Public Welfare Technology Application Research Project of Zhejiang Province of China (2016C31095), and the K.C. Wong Magna Fund of Ningbo University.

Author Contributions: Shengming Chang and Youming Li conceived and designed the entire procedure described in this paper and finished the CRLB analysis. Yucheng He assisted in performance comparisons between methods. Hui Wang performed the computer simulations and carried out the complexity analysis.

Conflicts of Interest: The authors declare no conflict of interest.

Abbreviations

The following abbreviations are used in this paper:

UWSN	Underwater Acoustic Wireless Sensor Network
UWA	Underwater Acoustic
RSS	Received Signal Strength
ToA	Time-of-Arrival
TDoA	Time-Different-of-Arrival
AoA	Angle-of-Arrival
SDP	Semi-Definite Programming
PDF	Probability Density Function
ML	Maximum Likelihood
WLS	Weighted Least Square
WLS-K	Weighted Least Square-Known
WLS-U	Weighted Least Square-Unknown
GTRS	Generalized Trust Region Subproblem
CRLBs	Cramer–Rao Lower Bounds
CRLB	Cramer–Rao Lower Bound
CRLB-K	Cramer–Rao Lower Bound-Known
CRLB-U	Cramer–Rao Lower Bound-Unknown
RMSE	Root Mean Square Error
Mc	Monte Carlo
CDF	Cumulative Density Function
ME	Mean Error

Appendix A. CRLBs Deduction

Appendix A.1. CRLB Deduction in the Known Target Transmit Power Case

In the known target transmit power case, according to the observation vectors $\boldsymbol{P} = [P_1, P_2, \cdots, P_N]^T (\boldsymbol{P} \in \mathbb{R}^N)$ in Equation (1), the condition PDF in the given $\boldsymbol{x}$ is

$$f(\boldsymbol{P}|\boldsymbol{x}) = \frac{1}{(2\pi)^{\frac{N}{2}}} \frac{1}{(|\boldsymbol{Q}|)^{\frac{1}{2}}} \exp\left\{-\frac{1}{2}\left(\boldsymbol{P} - \hat{\boldsymbol{P}}(\boldsymbol{x})\right)^T \boldsymbol{Q}^{-1}\left(\boldsymbol{P} - \hat{\boldsymbol{P}}(\boldsymbol{x})\right)\right\} \tag{A1}$$

where $\hat{\boldsymbol{P}}(\boldsymbol{x}) = [\hat{P}_1(\boldsymbol{x}), \cdots, \hat{P}_N(\boldsymbol{x})]^T$, and $\hat{P}_i(\boldsymbol{x}) = P_0 - 10\gamma \log_{10} \frac{\|\boldsymbol{x}-\boldsymbol{s}_i\|}{d_0} - \alpha_f(\|\boldsymbol{x} - \boldsymbol{s}_i\| - d_0), i = 1, \cdots, N$.

Thus, the log-likelihood function w.r.t the variable $\boldsymbol{x}$ has the following form

$$\ln f(\boldsymbol{P}|\boldsymbol{x}) = -\frac{N}{2}\ln(2\pi) - \frac{1}{2}\ln(|\boldsymbol{Q}|) - \frac{1}{2}\left(\boldsymbol{P} - \hat{\boldsymbol{P}}(\boldsymbol{x})\right)^T \boldsymbol{Q}^{-1}\left(\boldsymbol{P} - \hat{\boldsymbol{P}}(\boldsymbol{x})\right). \tag{A2}$$

For any unbiased estimator, i.e., $E(\widehat{x}) = x$, the covariance matrix $cov(\widehat{x})$ is lower bound by $cov(\widehat{x}) \geq J^{-1}$, where J is the Fisher information matrix (FIM). The CRLB is the inverse of FIM, J^{-1}, which can be derived from Equation (A2) as follows:

$$\frac{\partial \ln f(\boldsymbol{P}|\boldsymbol{x})}{\partial \boldsymbol{x}} = \left(\boldsymbol{P} - \hat{\boldsymbol{P}}(\boldsymbol{x})\right)^T \boldsymbol{Q}^{-1} \frac{\partial \hat{\boldsymbol{P}}(\boldsymbol{x})}{\partial \boldsymbol{x}}. \tag{A3}$$

Therefore,

$$\frac{\partial^2 \ln f(\boldsymbol{P}|\boldsymbol{x})}{\partial \boldsymbol{x} \partial \boldsymbol{x}^T} = -\left[\frac{\partial \hat{\boldsymbol{P}}(\boldsymbol{x})}{\partial \boldsymbol{x}}\right]^T \boldsymbol{Q}^{-1} \frac{\partial \hat{\boldsymbol{P}}(\boldsymbol{x})}{\partial \boldsymbol{x}} + \left(\boldsymbol{P} - \hat{\boldsymbol{P}}(\boldsymbol{x})\right)^T \boldsymbol{Q}^{-1} \frac{\partial \hat{\boldsymbol{P}}^2(\boldsymbol{x})}{\partial \boldsymbol{x} \partial \boldsymbol{x}^T}. \tag{A4}$$

Based on the assumption that n_i is a zero mean Gaussian random variable with the covariance matrix $\boldsymbol{Q}$, and taking the negative expectation on both sides of Equation (A4), we have

$$-E\left(\frac{\partial^2 \ln f(\boldsymbol{P}|\boldsymbol{x})}{\partial \boldsymbol{x} \partial \boldsymbol{x}^T}\right) = \left[\frac{\partial \hat{\boldsymbol{P}}(\boldsymbol{x})}{\partial \boldsymbol{x}}\right]^T \boldsymbol{Q}^{-1} \frac{\partial \hat{\boldsymbol{P}}(\boldsymbol{x})}{\partial \boldsymbol{x}} = \boldsymbol{G}^T \boldsymbol{Q}^{-1} \boldsymbol{G} \tag{A5}$$

where $\boldsymbol{G} = \frac{\partial \hat{\boldsymbol{P}}(\boldsymbol{x})}{\partial \boldsymbol{x}} = [g_1, g_2, \cdots, g_N]^T$ with

$$g_i = \frac{\partial \hat{P}_i(\boldsymbol{x})}{\partial \boldsymbol{x}} = -\frac{10\gamma}{\ln 10} \frac{(\boldsymbol{x} - \boldsymbol{s}_i)^T}{\|\boldsymbol{x} - \boldsymbol{s}_i\|^2} - \alpha_f \frac{(\boldsymbol{x} - \boldsymbol{s}_i)^T}{\|\boldsymbol{x} - \boldsymbol{s}_i\|}. \tag{A6}$$

Finally, we derive the closed-form expression of the CRLB in the known target transmit power case as

$$\text{CRLB-K} = \text{trace}(\boldsymbol{B}_1) \tag{A7}$$

where $\boldsymbol{B}_1 = (\boldsymbol{G}^T \boldsymbol{Q}^{-1} \boldsymbol{G})^{-1}$.

Appendix A.2. CRLB Deduction in the Unknown Target Transmit Power Case

According to the observation vectors $\boldsymbol{P} = [P_1, P_2, \cdots, P_N]^T (\boldsymbol{P} \in \mathbb{R}^N)$ given in Equation (1), the condition PDF of $\boldsymbol{z} = [\boldsymbol{x}^T; P_0]^T (\boldsymbol{z} \in \mathbb{R}^3)$ can be expressed as

$$f(\boldsymbol{P}|\boldsymbol{z}) = \frac{1}{(2\pi)^{\frac{N}{2}}} \frac{1}{(|\boldsymbol{Q}|)^{\frac{1}{2}}} \exp\left\{-\frac{1}{2}\left(\boldsymbol{P} - \hat{\boldsymbol{P}}(\boldsymbol{z})\right)^T \boldsymbol{Q}^{-1} \left(\boldsymbol{P} - \hat{\boldsymbol{P}}(\boldsymbol{z})\right)\right\} \tag{A8}$$

where $\hat{\boldsymbol{P}}(\boldsymbol{z}) = [\hat{P}_1(\boldsymbol{z}), f_2(\boldsymbol{z}), \cdots, \hat{P}_N(\boldsymbol{z})]^T$, and $\hat{P}_i(\boldsymbol{z}) = \boldsymbol{\iota}^T \boldsymbol{z} - 10\gamma \log_{10} \frac{\|\boldsymbol{F}^T \boldsymbol{z} - \boldsymbol{s}_i\|}{d_0} - \alpha_f(\|\boldsymbol{F}^T \boldsymbol{z} - \boldsymbol{s}_i\| - d_0), i = 1, \cdots, N$, $\boldsymbol{\iota} = [\boldsymbol{0}_{2\times 1}; 1]$, $\boldsymbol{F} = [\boldsymbol{I}_2; \boldsymbol{0}_{1\times 2}]$.

Similar as in Equation (A5), we have

$$-E\left(\frac{\partial^2 \ln f(\boldsymbol{P}|\boldsymbol{z})}{\partial \boldsymbol{z} \partial \boldsymbol{z}^T}\right) = \left[\frac{\partial \hat{\boldsymbol{P}}(\boldsymbol{z})}{\partial \boldsymbol{z}}\right]^T \boldsymbol{Q}^{-1} \frac{\partial \hat{\boldsymbol{P}}(\boldsymbol{z})}{\partial \boldsymbol{z}} = \boldsymbol{H}^T \boldsymbol{Q}^{-1} \boldsymbol{H} \tag{A9}$$

where $\boldsymbol{H} = \frac{\partial \hat{\boldsymbol{P}}(\boldsymbol{z})}{\partial \boldsymbol{z}} = [h_1, h_2, \cdots, h_N]^T$ with

$$h_i = \left[\frac{\partial \hat{P}_i(\boldsymbol{z})}{\partial \boldsymbol{x}}, \frac{\partial \hat{P}_i(\boldsymbol{z})}{\partial P_0}\right]^T = [-\frac{10\gamma}{\ln 10} \frac{(\boldsymbol{x} - \boldsymbol{s}_i)^T}{\|\boldsymbol{x} - \boldsymbol{s}_i\|^2} - \alpha_f \frac{(\boldsymbol{x} - \boldsymbol{s}_i)^T}{\|\boldsymbol{x} - \boldsymbol{s}_i\|}, 1]^T. \tag{A10}$$

Finally, we provide the closed-form expression of the CRLB in the unknown target transmit power case as

$$\text{CRLB-U} = \text{trace}(\boldsymbol{B}_2[1{:}2, 1{:}2]) \tag{A11}$$

where $\boldsymbol{B}_2 = (\boldsymbol{H}^T\boldsymbol{Q}^{-1}\boldsymbol{H})^{-1}$.

References

1. Akyildiz, I.F.; Su, W.; Sankarasubramaniam, Y.; Cayirci, E. Wireless sensor networks: A survey. *Comput. Netw.* **2002**, *38*, 393–422, doi:10.1016/S1389-1286(01)00302-4.
2. Garcia, M.; Sendra, S.; Atenas, M; Lloret, J. Underwater wireless ad-hoc networks: A survey. In *Mobile Ad Hoc Networks: Current Status and Future Trends*; CRC Press: Boca Raton, FL, USA; 2011; pp. 379–411.
3. Jaime, L. Underwater Sensor Nodes and Networks. *Sensors* **2013**, *13*, 11782–11796, doi:10.3390/s130911782.
4. Tan, H.P.; Diamant, R.; Seah, W.K.G.; Waldmeyer, M. A survey of techniques and challenges in underwater localization. *Ocean Eng.* **2011**, *38*, 1663–1676, doi:10.1016/j.oceaneng.2011.07.017.
5. Park, C.H.; Chang, J.H. Closed-form Two-step WLS-based TOA Source Localization Using Invariance Property of ML Estimator in Multiple-Sample Environment. *IET Commun.* **2016**, *10*, 1206–1213, doi:10.1049/iet-com.2015.0952.
6. Kim, S.; Cho, J.; Park, D. Moving-target position estimation using GPU-based particle filter for iot sensing applications. *Appl. Sci.* **2017**, *7*, 1152–1166, doi:10.3390/app7111152.
7. Rehan, K.; Qiao, G. A Survey of Underwater Acoustic Communication and Networking Techniques. *Res. J. Appl. Sci. Eng. Technol.* **2013**, *5*, 778–789.
8. Fang, X.; Nan, L.; Jiang, Z.; Chen, L. Multi-channel Fingerprint Localization Algorithm for Wireless Sensor Network in Multipath Environment. *IET Commun.* **2017**, *11*, 2253–2260, doi:10.1049/iet-com.2017.0429.
9. Hosseini, M.; Chizari, H.; Chai, K.S.; Budiarto, R. RSS-based distance measurement in Underwater Acoustic Sensor Networks: An application of the Lambert W function. In Proceedings of the International Conference on Signal Processing and Communication Systems, Gold Coast, Australia, 13–15 December 2011; pp. 1–4, doi:10.1109/ICSPCS.2010.5709656.
10. Kim, C.; Lee, S.; Kim, K. 3D underwater localization with hybrid ranging method for near-sea marine monitoring. In Proceedings of the International Conference Embedded and Ubiquitous Computing (EUC), Melbourne, Australia, 24–26 October 2011; pp. 438–441, doi:10.1109/EUC.2011.1.
11. Yan, Y.; Wang, W.; Shen, X.; Yang, F.; Chen, Z. Efficient convex optimization method for underwater passive source localization based on RSS with WSN. In Proceedings of the International Conference Signal Processing, Communication and Computing (ICSPCC), Hong Kong, China, 12–15 August 2012; pp. 171–174, doi:10.1109/ICSPCC.2012.6335673.
12. Xu, T.; Hu, Y.; Zhang, B.; Leus, G. RSS-Based Sensor Localization in Underwater Acoustic Sensor Networks. In Proceedings of the IEEE International Conference on Acoustics, Speech and Signal Processing (ICASSP), Shanghai, China, 20–25 March 2016; pp. 3906–3910, doi:10.1109/ICASSP.2016.7472409.
13. Wang, B.; Li, Y.; Huang, H.; Zhang, C. Target Localization in Underwater Acoustic Sensor Networks. In Proceedings of the Congress on Image and Signal Process, Sanya, China, 27–30 May 2008; Volume 4, pp. 68–72, doi:10.1109/CISP.2008.74.
14. More, J.J. Generalization of the Trust Region Problem. *Optim. Methods Soft* **1993**, *2*, 189–209, doi:10.1080/10556789308805542.
15. Tomic, S.; Beko, M.; Dinis, R. 3-D Target Localization in Wireless Sensor Network Using RSS and AoA Measurements. *IEEE Trans. Veh. Technol.* **2016**, *66*, 3197–3210, doi:10.1109/TVT.2016.2589923.
16. Brekhovskikh, L.M.; Lysanov, Y.P. Fundamentals of ocean acoustics (3rd edition). *J. Acoust. Soc. Am.* **2004**, *116*, 1863, doi:10.1016/0022-460X(92)90388-E.
17. Vaghefi, R.M.; Buehrer, R.M. Received Signal Strength-based Sensor Localization in Spatially Correlated Shadowing. In Proceedings of the IEEE International Conference on Acoustics, Speech and Signal Processing (ICASSP 2013), Vancouver, BC, Canada, 26–31 May 2013; pp. 4076–4080, doi:10.1109/ICASSP.2013.6638425.

18. Qarabaqi, P.; Stojanovic, M. Statistical characterization and computationally efficient modeling of a class of underwater acoustic communication channels. *IEEE J. Ocean. Eng.* **2013**, *38*, 701–717, doi:10.1109/JOE.2013.2278787.
19. Beck, A.; Stoica, P.; Li, J. Exact and approximate solutions of source localization problems. *IEEE Trans. Signal Process.* **2008**, *56*, 1770–1778, doi:10.1109/TSP.2007.909342.
20. Stojanovic, M. On the relationship between capacity and distance in an underwater acoustic communication channel. In Proceedings of the 1st ACM International Workshop on Underwater Networks, Los Angeles, CA, USA, 25 September 2006; ACM: New York, NY, USA; 2007; Vlume 11, pp. 34–43, doi:10.1145/1161039.1161049.
21. Stojanovic, M.; Preisig, J. Underwater acoustic communication channels: Propagation models and statistical characterization. *IEEE Commun. Mag.* **2009**, *47*, 84–89, doi:10.1109/MCOM.2009.4752682.
22. Cui, J.H.; Kong, J.; Gerla, M.; Zhou, S. The challenges of building mobile underwater wireless networks for aquatic applications. *IEEE Netw.* **2006**, *20*, 12–18, doi:10.1109/MNET.2006.1637927.
23. Pólik, I.; Terlaky, T. Interior Point Methods for Nonlinear Optimization. In *Nonlinear Optimization*, 1st ed.; Di Pillo, G., Schoen, F., Eds.; Springer: Berlin, Germany, 2010; Chapter 4, Volume 1989, pp. 215–276, doi:10.1007/978-3-642-11339-0.
24. Grant, M.; Boyd, S. CVX: Matlab Software for Disciplined Convex Programming. version 2.1. Available online: http://cvxr.com/cvx (accessed on 15 September 2014).
25. Sturm, J.F. Using SeDuMi 1.02, a MATLAB Toolbox for Optimization Over Symmetric Cones. *Opt. Methods Soft* **1999**, *11*, 625–653, doi:10.1080/10556789908805766.